photonics

MDPI

Communication

Optically Tunable Diffraction Efficiency in Reflection Grating Written in Photomobile Polymers

Riccardo Castagna [1,2], Andrea Di Donato [3], Oriano Francescangeli [4] and Daniele Eugenio Lucchetta [4,5,*]

[1] URT-CNR, Università di Camerino (UNICAM), Polo di Chimica, Via Sant'Agostino, 1, 62032 Camerino , Italy
[2] CNR, Institute of Heritage Science, Via Madonna del Piano, 10, 50019 Sesto Fiorentino, Italy
[3] Dip. DII, Università Politecnica delle Marche, Via Brecce Bianche, 60131 Ancona, Italy
[4] Dip. SIMAU, Università Politecnica delle Marche, Via Brecce Bianche, 60131 Ancona, Italy
[5] Optoacoustic Lab, Dip. SIMAU, Università Politecnica delle Marche, Via Brecce Bianche, 60131 Ancona, Italy
* Correspondence: d.e.lucchetta@univpm.it

Abstract: In this work, we report the fabrication and optical characterization of a one-dimensional reflection holographic volume phase grating recorded in a recently developed holographic photomobile composite polymer mixture. The reflection grating recorded on the photomobile material was a periodic one-dimensional arrangement of hard polymeric walls and viscous regions. The reflection notch was located in the near-infrared region of the electromagnetic spectrum. The transmission efficiency of the grating was modulated by an external CW laser light source operating at λ = 532 nm. The transmission efficiency increased with the increase in the power of the external laser source, and in the range of the used power values, the phenomenon was completely reversible. At the highest power levels, a 48% increase in the diffraction efficiency was achieved. The increase in the diffraction efficiency was related to the growth of the refractive-index contrast of the grating. In particular, under illumination, the viscous material escaped from the irradiated area. This feature explains the experimentally observed changes in the values of the grating's refractive index.

Keywords: photomobile polymers; lasers; tunability; diffraction efficiency; refractive index modulation

Citation: Castagna, R.; Di Donato, A.; Francescangeli, O.; Lucchetta, D.E. Optically Tunable Diffraction Efficiency in Reflection Grating Written in Photomobile Polymers. *Photonics* **2022**, *9*, 751. https://doi.org/10.3390/photonics9100751

Received: 9 August 2022
Accepted: 8 October 2022
Published: 11 October 2022

1. Introduction

Many optical devices are based on thin or thick holographic gratings or intermediate hybrid configurations [1–10]. Materials play an important role in the fabrication of holographic gratings, and their properties can be used to add functionalities to the recorded or self-assembled structures [11–14]. All-optically switchable volume holographic gratings have been studied for decades in several configurations and using a large variety of materials [15–27]. Optical switching can be found in mixtures containing azo dyes sensitive to the polarization state of the incident light. These dyes are mixed with liquid crystal (LC) molecules, and a change in the polarization state of the incident light results in a reorientation of the LC molecules in the system. The final result is a modification of the physical parameters characterizing the optical properties of the recorded periodic structures [28–37]. All-optical switching of highly nonlinear mixtures has also been exploited to modulate the optical properties of thin gratings when a static electric field is applied [25]. More recently, photomobile crystal polymer hybrid actuators [38] and azobenzene-based photomobile polymer thin films [39] were activated by light to generate and orient ripples on their surfaces. Other kinds of interesting light-actuated devices and sensors can be found in the literature [40–47]. Recently, we reported on the modulation of the optical properties of a transmission phase grating written in a novel holographic photomobile polymer mixture (H-PMP) [48]. H-PMP allows the production of polymer films that are holographic and photomobile at the same time [12,49]. In the present work, we wanted to miniaturize that optical system by realizing the phase grating in a guided configuration. For this reason, we used an H-PMP mixture where

a transmission grating working in reflection mode was recorded between two optical fibers. Such a configuration opens many opportunities in the fields of integrated optics and optical communications.

2. Materials and Methods

2.1. Materials

Camphorequinone (CQ), dipentaerythritol-monohydroxy-penta-acrylate (DPMHPA), 4-amino-phenol (4-AP), tri-phenyl-o-methane-tri-glycidil-ether (TPMTGE), [phenyl-(2,4,6-trimethylbenzoyl) phosphoryl]-(2,4,6-trimethylphenyl) methanone (PTPTM), N-Vinyl butyrolactam (NVBL), and Lead(IV) oxide (PbO_2) were purchased from Merck, Darmstadt, Germany.

2.2. Holographic Mixture Preparation

The mixture was prepared starting with the recipe published in [12], to which we added the epoxide monomer TPMTGE and the photoinitiator CQ. The monomers used were TPMTGE:DPMHPA:NVBL (0.1:2:5, molar ratio); the photoinitiators used were CQ:PTPTM (0.1:0.1 molar ratio) and 4-AP:PbO_2 (1:0.5 molar ratio). The reaction between the PbO_2, NVBL, and 4-AP was conducted at room temperature for one week under magnetic stirring. After that, the resulting mixture was left to rest in the dark for one week. Separately, acrylate was mixed with liquid TPMTGE and heated at the temperature of 90 °C. The mixture remained under mechanical stirring until a pale yellow color was obtained. The content of the bottle was mixed with the reaction containing NVBL, 4-AP, and PbO2, and the final mixture remained under magnetic stirring for a further 36 h. The initiators were then added to the system. At this stage, the mixture remained under magnetic stirring for a further 24 h. The addition of a synergic two photoinitiator system allowed the polymerization in the visible range at $\lambda = 532$ nm. Further details on the mixture preparation can be found in ref. [48].

2.3. Recording, Pumping, and Data Acquisition Setups

An optical fiber (OF) with an internal diameter of 100 µm was inserted between two microscope glasses containing the H-PMP mixture. The OF was cut into two parts, and a transmission grating working in reflection mode was recorded between the two fibers using the setup depicted in Figures 1 and 2. With a writing angle $\theta = 70°$ and a refractive index of the H-PMP mixture of 1.58, the notch of the recorded grating observed in the reflection mode was at $\lambda > 880$ nm. The written hologram was optically characterized by using a large band Xe light source and a real time spectrometer. The external CW pumping light was a DPSS light source at $\lambda = 532$ nm, which impinged on the grating at different powers. The light-induced changes in the optical properties of the recorded structure were detected in real time and analyzed. Filters were used to remove any influence on the recorded spectra due to the presence of the external light source.

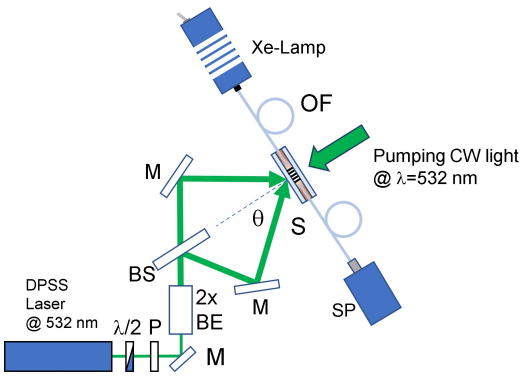

Figure 1. Sketch of the writing, pumping, and detecting setup. $\lambda/2$ = half wavelength plate; P = polarizer; M = Mirror; 2x BE = 2x Beam Expander; BS = Beam Splitter; S = sample; OF = Optical Fiber; SP = Spectrometer.

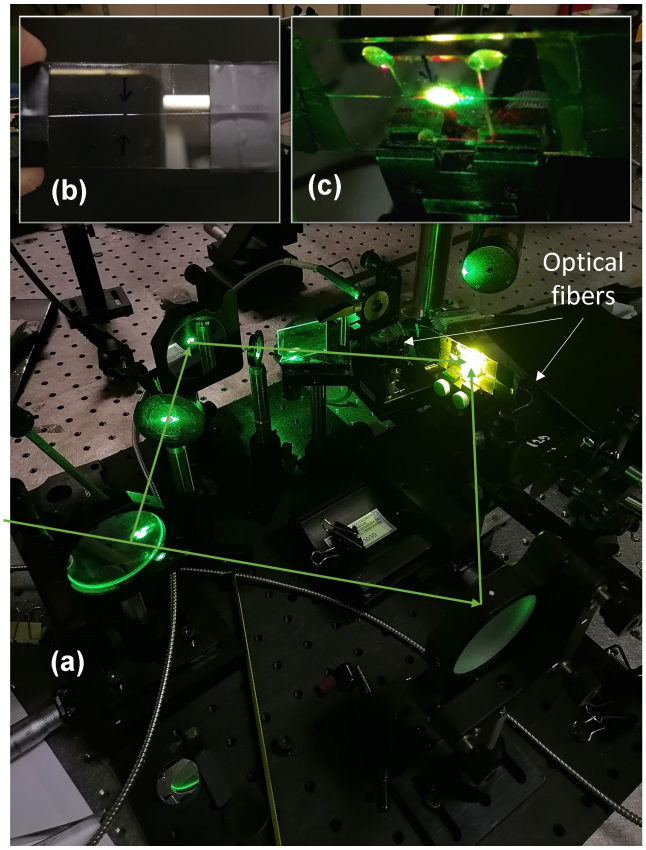

Figure 2. (**a**) The experimental setup used to record the holograms. The insets show the sample without the covering glass (**b**) and during irradiation (**c**).

3. Results and Discusssion

Figure 3 shows a typical reflection peak recorded in our samples. The diffraction (reflection) efficiency was ≈30 %. The reflection efficiency was relatively low due to the reflection losses connected with the wide recording angle, the light scattering from the edges of the optical fibers, and the impurities inside the samples. Figure 2a shows the real experimental setup. The green arrows represent the writing beams. The insets show the main steps of the sample fabrication. Figure 2b shows the empty cell and the alignment of the optical fibers, and Figure 2c shows the two glasses cell filled with the H-PMP mixture during the irradiation process.

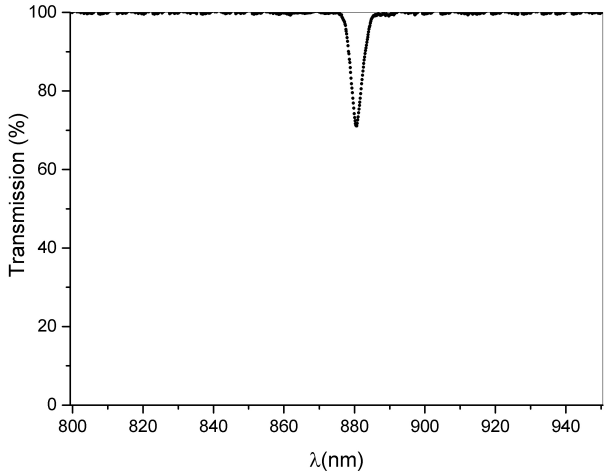

Figure 3. Normalized transmission spectrum recorded with a laser power P = 150 mW per beam and a recording wavelength λ = 532 nm.

By irradiating the sample with an external light source, the measured values of the diffraction efficiency increased, as shown in Figure 4.

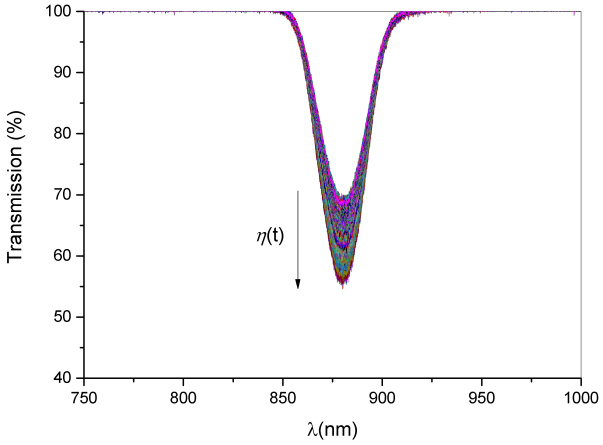

Figure 4. Dynamical behavior of the transmission spectra under external irradiation at λ = 532 nm and P = 240 mW. The diffraction efficiency increased by 48%. Irradiation time t = 30 s.

The diffraction efficiency of a one-dimensional reflection phase grating can be written as:

$$\eta(d) = e^{-2\alpha d} \frac{tanh\left(\sqrt{(\nu^2 + \xi^2)}\right)^2}{1 + \frac{\xi^2}{\nu^2}} \tag{1}$$

Respectively, the coupling and detuning parameters are defined as:

$$\nu = \frac{\pi \Delta n d}{\lambda cos(\theta)} \tag{2}$$

$$\xi = \Delta\theta \beta d sin(\theta_B). \tag{3}$$

where Δn is the induced refractive index variation, d is the grating thickness, λ is the reading wavelength in the free space, θ is the angle of incidence, θ_B is the Bragg angle, $\Delta\theta = \theta - \theta_B$, n is the average refractive index of the medium, and $\beta = 2\pi n/\lambda$. The parameter $\Delta\theta$ in Equation (3) describes the dephasing term appearing when λ or θ are varied. Their connection is given by the following equation in which the grating period Λ appears explicitly:

$$\Delta\theta = \frac{2\pi}{\Lambda} \cdot \sin\theta - \left(\frac{2\pi}{\Lambda}\right)^2 \frac{\lambda}{4 \cdot \pi \cdot n} \tag{4}$$

Under the Bragg condition $\Delta\theta = 0$, the Equation (4) takes the well-known expression:

$$\theta_0(\lambda) = \arcsin\left(\frac{\lambda}{2 \cdot \Lambda \cdot n}\right), \tag{5}$$

which leads to the following expression for the diffraction efficiency:

$$\eta(\lambda, \Delta n) = e^{-\frac{2\alpha d}{\cos\theta_0(\lambda)}} \tanh^2\left(\frac{\pi \cdot \Delta n \cdot d}{\lambda \cos\theta_0(\lambda)}\right) \tag{6}$$

Assuming an absorption coefficient α, independent of the working wavelength λ and intensity of the pumping laser applied to the sample, we can derive from Equation (6) the refractive index deviation δn as a function of the diffraction efficiency at the measured wavelength λ, as follows:

$$\delta n = \frac{\lambda \cos\theta_0(\lambda)}{\pi \cdot d} \text{atanh}\left(e^{\frac{\alpha d}{\cos\theta_0(\lambda)}} \sqrt{\eta(\lambda)}\right) \tag{7}$$

Equation (7) is the nonlinear analytical relationship between the diffraction efficiency and the refractive index contrast. It clearly states that the increase in the diffraction efficiency under the pumping illumination is related to the corresponding changes in the refractive index modulation Δn. The above equation is used to derive the dynamical behavior of the refractive index deviation at different power levels of the external laser source, as shown in Figure 5. After a proper data normalization, which accounted for the grating response at rest without external pumping, the diffraction efficiency was computed and used to derive the refractive index deviation Δn, according to the Equation (7). Figure 5 shows the behavior of the refractive index modulation Δn as a function of time when the grating is illuminated for ≈30 s at λ = 532 nm with different power levels ranging from 30 to 240 mW. The irradiated area overlapped the entire grating surface. For the used powers, we always observed a reversible increase in the diffraction efficiency during irradiation.

Reflection holograms are, at time of writing, impossible to record in H-PMP polymer films. To overcome this limitation, different approaches can be used. As an example, in the recent past, we recorded a high-resolution reflection hologram in a well known holographic mixture and successfully attached it to an H-PMP film. The approach used in this work is different, because we recorded the one dimensional hologram in transmission mode and used it in reflection mode. In this guided configuration, regardless of the power used during the irradiation process, the diffraction efficiency increased in time up to a maximum value and relaxed to the initial value when the external laser was switched off. By inverting the growing curve, the resulting curve completely overlapped the shape of the decay curve. This evidenced that the physical phenomenon governing the excitation and relaxation behaviors was the same. In order to explain the detected changes in the diffracted efficiency during irradiation, we recall the photophobic nature of the used compounds [12,50]. During the irradiation process, the doped-NVBL escaped from the irradiated area, and as a consequence, the grating refractive index modulation increased. The reverse occurred when the pump laser was turned off [48,51]. Our hypothesis is that this property plays the main role when considering the dynamic behavior of our grating under light irradiation.

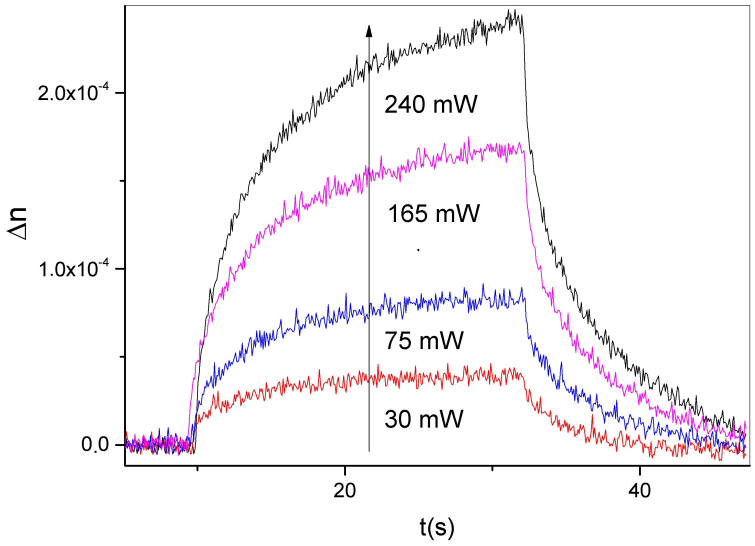

Figure 5. Refractive index modulation Δn as a function of time for different irradiation power levels, from 30 mW to 240 mW.

4. Conclusions

In this work, we reported on the fabrication and optical characterization of a one-dimensional reflection holographic volume phase grating written in a PMP mixture. The reflection grating recorded in the photomobile material was a periodic one-dimensional arrangement of hard polymeric walls and low viscous regions and showed a reflection

peak located in the near-infrared region of the electromagnetic spectrum. The depth of the reflection peak was modulated by an external DPSS CW laser light source operating at $\lambda = 532$ nm. In particular, the transmission efficiency increased with the power of the external laser source. For low power values, the phenomenon was completely reversible. The increase in the diffraction efficiency was related to the changes in the refractive-index modulation of the grating. In particular, under illumination, the low viscous material escaped from the irradiated area, and the index modulation δn increased. The observed nonlinear optical response can be helpful for optical limiting applications [52] and sensing [53,54].

Author Contributions: Conceptualization, R.C. and D.E.L.; methodology, R.C. and D.E.L.; software, A.D.D.; validation, R.C. and D.E.L.; formal analysis, A.D.D.; investigation, R.C. and D.E.L.; resources, R.C.; writing—original draft preparation, R.C. and D.E.L.; writing—review and editing, D.E.L., R.C., A.D.D. and O.F.; supervision, O.F.; project administration, R.C.; funding acquisition, R.C. All authors have read and agreed to the published version of the manuscript.

Funding: R.C. thanks the "Marche Applied Research Laboratory for Innovative Composites" (MARLIC), POR Marche FESR 2014–2020, Regione Marche (Italy).

Institutional Review Board Statement: Not applicable.

Informed Consent Statement: Not applicable.

Data Availability Statement: Data are available from the authors under reasonable request.

Acknowledgments: R.C. acknowledges the support of "Marche Applied Research Laboratory for Innovative Composites" (MARLIC), POR Marche FESR 2014–2020, Regione Marche (Italy).

Conflicts of Interest: The authors declare no conflicts of interest.

References

1. Lucchetta, D.; Spegni, P.; Di Donato, A.; Simoni, F.; Castagna, R. Hybrid surface-relief/volume one dimensional holographic gratings. *Opt. Mater.* **2015**, *42*, 366–369. [CrossRef]
2. Shishova, M.; Zherdev, A.; Lushnikov, D.; Odinokov, S. Recording of the Multiplexed Bragg Diffraction Gratings for Waveguides Using Phase Mask. *Photonics* **2020**, *7*, 97. [CrossRef]
3. Shishova, M.; Zherdev, A.; Odinokov, S.; Venediktov, V.; Lushnikov, D.; Kim, Y. Selective Couplers Based on Multiplexed Volume Holographic Gratings for Waveguide Displays. *Photonics* **2021**, *8*, 232. [CrossRef]
4. Park, T.H.; Kim, S.M.; Oh, M.C. Polymer-waveguide Bragg-grating devices fabricated using phase-mask lithography. *Curr. Opt. Photonics* **2019**, *3*, 401–407.
5. Lucchetta, D.; Vita, F.; Francescangeli, D.; Francescangeli, O.; Simoni, F. Optical measurement of flow rate in a microfluidic channel. *Microfluid. Nanofluidics* **2016**, *20*, 1–5. [CrossRef]
6. Wu, P.F; Wu, Z.J.; Zhuang, Y.; Liu, H.L. Holographic grating fabrication for wide angular bandwidth using polymer thin films. *Optoelectron. Lett.* **2021**, *17*, 1–4. [CrossRef]
7. Tomita, Y.; Aoi, T.; Hasegawa, S.; Xia, F.; Wang, Y.; Oshima, J. Very high contrast volume holographic gratings recorded in photopolymerizable nanocomposite materials. *Opt. Express* **2020**, *28*, 28366–28382. [CrossRef] [PubMed]
8. Narita, A.; Oshima, J.; Iso, Y.; Hasegawa, S.; Tomita, Y. Red-sensitive organic nanoparticle-polymer composite materials for volume holographic gratings with large refractive index modulation amplitudes. *Opt. Mater. Express* **2021**, *11*, 614–628. [CrossRef]
9. Liu, H.; Wang, R.; Yu, D.; Luo, S.; Li, L.; Wang, W.; Song, Q. Direct light written holographic volume grating as a novel optical platform for sensing characterization of solution. *Opt. Laser Technol.* **2019**, *109*, 510–517. [CrossRef]
10. Zheng, H.; Zhou, Y.; Ugwu, C.F.; Du, A.; Kravchenko, I.I.; Valentine, J.G. Large-Scale Metasurfaces Based on Grayscale Nanosphere Lithography. *ACS Photonics* **2021**, *8*, 1824–1831. [CrossRef]
11. Vita, F.; Lucchetta, D.E.; Castagna, R.; Criante, L.; Simoni, F. Effects of resin addition on holographic polymer dispersed liquid crystals. *J. Opt. Pure Appl. Opt.* **2009**, *11*, 024021. [CrossRef]
12. Castagna, R.; Nucara, L.; Simoni, F.; Greci, L.; Rippa, M.; Petti, L.; Lucchetta, D.E. An Unconventional Approach to Photomobile Composite Polymer Films. *Adv. Mater.* **2017**, *29*, 1604800. [CrossRef]
13. Shalit, A.; Lucchetta, D.; Piazza, V.; Simoni, F.; Bizzarri, R.; Castagna, R. Polarization-dependent laser-light structured directionality with polymer composite materials. *Mater. Lett.* **2012**, *81*, 232–234. [CrossRef]
14. Lucchetta, D.; Simoni, F.; Hernandez, R.; Mazzulla, A.; Cipparrone, G. Lasing from chiral doped nematic liquid crystal droplets generated in a microfluidic device. *Mol. Cryst. Liq. Cryst.* **2017**, *649*, 11–19. [CrossRef]
15. White, T.J.; Tabiryan, N.V.; Serak, S.V.; Hrozhyk, U.A.; Tondiglia, V.P.; Koerner, H.; Vaia, R.A.; Bunning, T.J. A high frequency photodriven polymer oscillator. *Soft Matter* **2008**, *4*, 1796–1798. [CrossRef]

16. Francescangeli, O.; Lucchetta, D.E.; Slussarenko, S.S.; Reznikov, Y.A.; Simoni, F. Light-controlled anchoring energy in nematic liquid crystals. *Mol. Cryst. Liq. Cryst. Sci. Technol. Sect. Mol. Cryst. Liq. Cryst.* **2001**, *360*, 193–201. [CrossRef]
17. Chang, W.T.; Cheng, C.L.; Li, Y.J.; Wang, T.H.; Kuo, M.Y.; Hsiao, V.K. All-optical switching in holographic polymer dispersed azobenzene liquid-crystal gratings. In *Proceedings of the Practical Holography XXIII: Materials and Applications*; International Society for Optics and Photonics: Bellingham, WA, USA, 3 February 2009; Volume 7233, p. 72330X.
18. De Sio, L.; Veltri, A.; Umeton, C.; Serak, S.; Tabiryan, N. All-optical switching of holographic gratings made of polymer-liquid-crystal-polymer slices containing azo-compounds. *Appl. Phys. Lett.* **2008**, *93*, 181115. [CrossRef]
19. Su, Y.C.; Chu, C.C.; Chang, W.T.; Hsiao, V. Characterization of optically switchable holographic polymer-dispersed liquid crystal transmission gratings. *Opt. Mater.* **2011**, *34*, 251–255. [CrossRef]
20. De Sio, L.; Umeton, C.; Serak, S.; Tabiryan, N. Full Optical Control of Holographic Gratings Realized in Composite Materials Containing Photosensitive Liquid Crystals. *Mol. Cryst. Liq. Cryst.* **2010**, *526*, 101–107. [CrossRef]
21. De Sio, L.; Cuennet, J.G.; Vasdekis, A.E.; Psaltis, D. All-optical switching in an optofluidic polydimethylsiloxane: Liquid crystal grating defined by cast-molding. *Appl. Phys. Lett.* **2010**, *96*, 131112. [CrossRef]
22. Tong, X.; Wang, G.; Yavrian, A.; Galstian, T.; Zhao, Y. Dual-Mode Switching of Diffraction Gratings Based on Azobenzene-Polymer-Stabilized Liquid Crystals. *Adv. Mater.* **2005**, *17*, 370–374. [CrossRef]
23. Bang, C.U.; Shishido, A.; Ikeda, T. Azobenzene Liquid-Crystalline Polymer for Optical Switching of Grating Waveguide Couplers with a Flat Surface. *Macromol. Rapid Commun.* **2007**, *28*, 1040–1044. [CrossRef]
24. De Sio, L.; Serak, S.; Tabiryan, N.; Ferjani, S.; Veltri, A.; Umeton, C. Composite Holographic Gratings Containing Light-Responsive Liquid Crystals for Visible Bichromatic Switching. *Adv. Mater.* **2010**, *22*, 2316–2319. [CrossRef]
25. Lucchetta, D.; Vita, F.; Simoni, F. All-optical switching of diffraction gratings infiltrated with dye-doped liquid crystals. *Appl. Phys. Lett.* **2010**, *97*, 231112. [CrossRef]
26. Castagna, R.; Lucchetta, D.E.; Rippa, M.; Xu, J.H.; Donato, A.D. Near-frequency photons Y-splitter. *Appl. Mater. Today* **2020**, *19*, 636. [CrossRef]
27. Fenoll, S.; Brocal, F.; Segura, J.D.; Ortuño, M.; Beléndez, A.; Pascual, I. Holographic characteristics of photopolymers containing different mixtures of nematic liquid crystals. *Polymers* **2019**, *11*, 325. [CrossRef]
28. Stoilova, A.; Mateev, G.; Nazarova, D.; Nedelchev, L.; Stoykova, E.; Blagoeva, B.; Berberova, N.; Georgieva, S.; Todorov, P. Polarization holographic gratings in PAZO polymer films doped with particles of biometals. *J. Photochem. Photobiol. A Chem.* **2021**, *411*, 113196. [CrossRef]
29. Ahmad, A.; Alsaad, A.; Al-Bataineh, Q.M.; Al-Akhras, M.A.H.; Albataineh, Z.; Alizzy, K.A.; Daoud, N.S. Synthesis and characterization of ZnO NPs-doped PMMA-BDK-MR polymer-coated thin films with UV curing for optical data storage applications. *Polymer Bull.* **2020**, *78*, 1189–1211. [CrossRef]
30. Alsaad, A.; Al-Bataineh, Q.M.; Telfah, M.; Ahmad, A.; Albataineh, Z.; Telfah, A. Optical properties and photo-isomerization processes of PMMA–BDK–MR nanocomposite thin films doped by silica nanoparticles. *Polymer Bull.* **2020**, *78*, 3425–3441. [CrossRef]
31. Nedelchev, L.; Ivanov, D.; Blagoeva, B.; Nazarova, D. Optical anisotropy induced at five different wavelengths in azopolymer thin films: Kinetics and spectral dependence. *J. Photochem. Photobiol. A Chem.* **2019**, *376*, 1–6. [CrossRef]
32. Mateev, G.; Stoilova, A.; Nazarova, D.; Nedelchev, L.; Todorov, P.; Georgieva, S.; Trifonova, Y.; Lilova, V. Photoinduced Birefringence in azo Polymer Nanocomposite Films with Embedded Particles of Biologically Aactive MetalL Complexes. *J. Chem. Technol. Metall.* **2019**, *54*, 1123–1127.
33. Loşmanskii, C.; Achimova, E.; Abaskin, V.; Meshalkin, A.; Prisacar, A.; Loghina, L.; Vlcek, M.; Yakovleva, A. QDs doped azopolymer for direct holographic recording. In Proceedings of the International Conference on Nanotechnologies and Biomedical Engineering, Chisinau, Moldova, 3–5 November 2019; Springer: Berlin/Heidelberg, Germany, 2019; pp. 275–278.
34. Neipp, C.; Taleb, S.I.; Francés, J.; Fernández, R.; Puerto, D.; Calzado, E.M.; Gallego, S.; Beléndez, A. Analysis of the Imaging Characteristics of Holographic Waveguides Recorded in Photopolymers. *Polymers* **2020**, *12*, 1485. [CrossRef] [PubMed]
35. Bugakov, M.; Sakhno, O.; Boiko, N.; Ryabchun, A. Polarization Gratings in Azobenzene-Based Fully Liquid Crystalline Triblock Copolymer. *Macromol. Rapid Commun.* **2019**, *40*, 1900412. [CrossRef]
36. Vorzobova, N.; Sokolov, P. Application of Photopolymer Materials in Holographic Technologies. *Polymers* **2019**, *11*, 2020. [CrossRef]
37. Tien, C.L.; Lin, R.J.; Kang, C.C.; Huang, B.Y.; Kuo, C.T.; Huang, S.Y. Electrically controlled diffraction grating in azo dye-doped liquid crystals. *Polymers* **2019**, *11*, 1051. [CrossRef]
38. Hasebe, S.; Matsuura, D.; Mizukawa, T.; Asahi, T.; Koshima, H. Light-Driven Crystal–Polymer Hybrid Actuators. *Front. Robot. AI* **2021**, *8*, 141. [CrossRef]
39. Koskela, J.E.; Vapaavuori, J.; Ras, R.H.; Priimagi, A. Light-driven surface patterning of supramolecular polymers with extremely low concentration of photoactive molecules. *ACS Macro Lett.* **2014**, *3*, 1196–1200. [CrossRef]
40. Hagiwara, Y.; Taniguchi, T.; Asahi, T.; Koshima, H. Crystal actuator based on a thermal phase transition and photothermal effect. *J. Mater. Chem. C* **2020**, *8*, 4876–4884. [CrossRef]
41. Majidi, C. Soft-matter engineering for soft robotics. *Adv. Mater. Technol.* **2019**, *4*, 1800477. [CrossRef]
42. Naumov, P.; Karothu, D.P.; Ahmed, E.; Catalano, L.; Commins, P.; Mahmoud Halabi, J.; Al-Handawi, M.B.; Li, L. The Rise of the Dynamic Crystals. *J. Am. Chem. Soc.* **2020**, *142*, 13256–13272. [CrossRef]

43. Taniguchi, T.; Asahi, T.; Koshima, H. Photomechanical azobenzene crystals. *Crystals* **2019**, *9*, 437. [CrossRef]
44. Fumoto, T.; Miho, S.; Mise, Y.; Imato, K.; Ooyama, Y. Polymer films doped with fluorescent sensor for moisture and water droplet based on photo-induced electron transfer. *RSC Adv.* **2021**, *11*, 17046–17050. [CrossRef] [PubMed]
45. Azmoudeh, E.; Farazi, S. Ultrafast and low power all-optical switching in the mid-infrared region based on nonlinear highly doped semiconductor hyperbolic metamaterials. *Opt. Express* **2021**, *29*, 13504–13517. [CrossRef] [PubMed]
46. Castagna, R.; Lucchetta, D.E.; Vita, F.; Criante, L.; Simoni, F. At a glance determination of laser light polarization state. *Appl. Phys. Lett.* **2008**, *92*. [CrossRef]
47. Lucchetta, D.E.; Castagna, R.; Simoni, F. Light-actuated contactless macro motors exploiting Bénard–Marangoni convection. *Opt. Express* **2019**, *27*, 13574–13580. [CrossRef]
48. Lucchetta, D.E.; Di Donato, A.; Singh, G.; Tombesi, A.; Castagna, R. Optically tunable diffraction efficiency by photo-mobile holographic composite polymer material. *Opt. Mater.* **2021**, *121*, 111612. [CrossRef]
49. Castagna, R.; Vita, F.; Lucchetta, D.E.; Criante, L.; Simoni, F. Superior-Performance Polymeric Composite Materials for High-Density Optical Data Storage. *Adv. Mater.* **2009**, *21*, 589–592. [CrossRef]
50. Lucchetta, D.E.; Di Donato, A.; Paturzo, M.; Singh, G.; Castagna, R. Light-Induced Dynamic Holography. *Micromachines* **2022**, *13*, 297. [CrossRef]
51. Lucchetta, D.E.; Castagna, R.; Singh, G.; Riminesi, C.; Di Donato, A. Spectral, morphological and dynamical analysis of a holographic grating recorded in a photo-mobile composite polymer mixture. *Nanomaterials* **2021**, *11*, 2925. [CrossRef]
52. Guddala, S.; Ramakrishna, S.A. Optical limiting by nonlinear tuning of resonance in metamaterial absorbers. *Opt. Lett.* **2016**, *41*, 5150–5153. [CrossRef]
53. Guddala, S.; Kumar, R.; Ramakrishna, S.A. Thermally induced nonlinear optical absorption in metamaterial perfect absorbers. *Appl. Phys. Lett.* **2015**, *106*, 111901. [CrossRef]
54. Guddala, S.; Rao, D.N.; Ramakrishna, S.A. Resonant enhancement of Raman scattering in metamaterials with hybrid electromagnetic and plasmonic resonances. *J. Opt.* **2016**, *18*, 065104. [CrossRef]